RSC Advances

This is an *Accepted Manuscript*, which has been through the Royal Society of Chemistry peer review process and has been accepted for publication.

Accepted Manuscripts are published online shortly after acceptance, before technical editing, formatting and proof reading. Using this free service, authors can make their results available to the community, in citable form, before we publish the edited article. This *Accepted Manuscript* will be replaced by the edited, formatted and paginated article as soon as this is available.

You can find more information about *Accepted Manuscripts* in the **Information for Authors**.

ROYAL SOCIETY OF CHEMISTRY

www.rsc.org/advances

Synergistic Photothermal Antimicrobial Therapy using Graphene Oxide/Polymer Composite Layer-by-Layer Thin Films

Rajendra Kurapati,[a] Mahalakshmi Vaidyanathan,[a] Ashok M Raichur[a b]*

[a] Department of Materials Engineering, Indian Institute of Science, Bangalore, India 560012

[b] Nanotechnology and Water Sustainability Research Unit, University of South Africa, Science Campus, Florida, 1709, Johannesburg

Corresponding author: amr@materials.iisc.ernet.in

Keywords: layer-by-layer self-assembly, graphene oxide, thin films, photothermal therapy, antimicrobial coatings

Abstract

We report an efficient and a simple synergistic antimicrobial therapy for lysing of pathogenic *E. coli K12 MG1655* using layer-by-layer (LbL) films of graphene oxide (GO) and poly(allylamine hydrochloride) (PAH). Two kinds of antimicrobial therapies have been tested in this study. The first therapy involves the inherent antimicrobial property of GO studied by incubating the bacteria with glass slides coated with GO/PAH films up to 16 h (varying number of layers from 20 to 80). The optical density (OD) measurements at 600 nm revealed that antimicrobial activity of the films increased with increase in number of layers, which can be attributed to increase in the roughness of the films and also the amount of GO in the films. The second therapy involves exploiting the photothermal property of GO by exposing the films to near-infrared (NIR) laser at 1064 nm (Nd:YAG, 10 ns pulse, 10 Hz, 85 mW) for 15 min and incubation for 4 or 16 h. The photothermal therapy results revealed the enhanced antimicrobial activity compared to incubation of bacteria with films in the absence of NIR-laser for 4 or 16 h. The enhanced antimicrobial activity of GO/PAH films is because of the synergistic effect resulting from membrane-stress induced on bacteria by GO sheets and photothermal heating in the presence of NIR-light. Further, we have also performed fluorescence-based live/dead assay using confocal fluorescence microscopy to verify the viability of bacterial cells after incubating the bacteria and GO/PAH films with and without NIR laser. All the results suggest that the synergistic antimicrobial effect of GO/PAH films causes increased lysis of *E. coli* compared to the individual effects.

Introduction

In recent times, the development of high efficient methods for killing multidrug-resistant bacteria have gained tremendous research interest, due to increase in the prevalence of antibiotic-resistant bacteria.[1] Development of alternative methods for killing pathogenic bacteria is one of the biggest challenges in biomedical research. Several nanotechnology-driven composite materials such as silver, copper, ZnO, MgO, TiO_2, etc. have attracted enormous attention in antimicrobial applications over traditional antibiotic drugs.[2, 3] More recently, near infrared (NIR) light guiding photothermal therapy (PTT) has been explored as an attractive alternative technique for killing of pathogenic bacteria. PTT involves generation of heat from the photothermal agents due to NIR-light exposure, which causes irreparable damage to the cell-membrane and eventually causing cell death.[4] So far, various gold nanoparticles (NPs) [2, 5, 6] and carbon nanotubes (CNTs) based composite materials have been used for PTT.[7]

Currently graphene oxide (GO), a derivative of graphene, has received a great deal of attention and emerged as a key nanomaterial for various industrial and biomedical applications due to its superior mechanical and optical properties.[8, 9] Because of its superior solubility and amphiphilic nature over native graphene, various potential applications of GO in biosensors, bio-imaging, drug/gene delivery have been investigated.[10-16] In addition, GO[17] and composites of GO with Ag,[17, 18] TiO_2,[19] various polymers[20-23] and dye[24] demonstrate excellent antimicrobial properties. Further, based on the photothermal conversion ability of GO upon NIR light exposure,[25] PTT for killing various tumour cells and pathogenic bacteria have been reported.[26-28]

Over a last decade, layer-by-layer (LbL) self-assembly of polyelectrolytes for fabrication of thin films or hollow capsules has been a subject of intensive research for various biomedical applications (e.g. drug delivery, cell adhesive materials, etc.).[29] Due to versatility in the LbL self-assembly, various kinds of materials such as nanoparticles, dendrimers, charged small molecules, micelles, carbon nanotubes, fullerenes, etc. can be incorporated in the LbL films along with polyelectrolytes. By using hybrid LbL films, antimicrobial properties were imparted to the films by incorporation of antimicrobial peptides,[30] Ag NPs,[31, 32] and CNTs.[33] Over the past few years, our group has utilized the unique advantages of GO by incorporating the same into LbL films for potential biomedical applications like dual-drug delivery and NIR light responsive drug release, etc.[10, 11, 34-37] Thus, so far the two properties of GO i.e. photothermal therapy and antimicrobial property have been individually studied. It would be more interesting and versatile to combine

the antimicrobial and photothermal properties of GO in the form of LbL films for enhanced killing of pathogenic bacteria in a synergistic way. Moreover, these LbL films could be coated easily irrespective of the substrate unlike LB films. Langmuir-Blodgett (LB) films of GO have also shown antimicrobial properties.[23, 38] More recently, Kim and co-workers have demonstrated an excellent sensitization method for bacteria by using highly flexible and hybrid LbL films of GO and 2D titanate nanosheets and these films displayed a complete sterilization of *E. coli* within 15 min.[39]

In this work, we have fabricated composite multilayer thin films of GO with polymer PAH by the LbL technique. Using these GO/PAH composite films, we have studied the antimicrobial activity of films with and without NIR-laser light (PTT) with *E. coli* culture as a model microorganism. By increasing the number of layers of films, antimicrobial activity was enhanced gradually. Photothermal killing of bacteria was achieved by exposing the films to a very low power pulse NIR-laser (Nd:YAG, 10 ns pulse, 85 mW). Finally, we observed that the synergistic antimicrobial activity obtained by combining the membrane stress induced by GO sheets and photothermal heating due to NIR-light exposure of GO resulted in more cell death when compared to the individual processes.

2. Experimental Section

2.1: Materials

High purity graphite powder with average grain size 45 μm, PAH (M_w = 70 kDa) and $KMnO_4$ were purchased from Sigma-Aldrich and used without further purification. H_2SO_4, HCl, $NaNO_2$, NaOH, $NaNO_3$ and glass slides were purchased from SRL India. Water used in all the experiments was obtained from Milli-Q system with resistivity greater than 18 MΩ cm. Tryptone type − I, yeast extract powder and bacto agar were purchased from Hi-Media Labs. Sodium chloride, 1,4-diazobicyclooctane (DAPI), propidium iodide (PI) solution, glutaraldehyde, phosphate buffered saline (PBS) tablets were all purchased from Sigma-Aldrich and used without any further purification. Millipore water (18 MΩ resistivity) was used for rinsing/washing films. For pH adjustments, 0.1 M HCl/NaOH solutions prepared in DI water were used.

2.2: Synthesis of exfoliated graphene oxide (GO)

The fully exfoliated GO was synthesized by using modified-Hummer's method followed by ultrasonication.[40, 41] Initially, 46 mL of H_2SO_4 (98%) was added to 2 g of graphite powder (45 μm, Sigma-Aldrich) in a flask and stirred for 8 h, followed by addition of 6 g of $KMnO_4$ slowly to above mixture while keeping the temperature below 20 ^{0}C. Next, distilled water was added to dilute the mixture and heated at 100 ^{0}C for 30 min. Then 350 mL of distilled water was gradually added and temperature was kept below 100 ^{o}C. Finally, the reaction was terminated by adding 20 mL of H_2O_2 (30%) and 300 mL of distilled water. Slowly, the colour of the dispersion turned from dark brown to yellow. Several repeated centrifugations (8000 rpm for 25 min) were carried out to wash the mixture using 5% HCl and distilled water. The mixture was then subjected to dialysis to get rid of residual salts, acids and metal ions from the graphite oxide suspension. The exfoliated graphene oxide was obtained by ultrasonication (Soniclean, 160 HT, 170W, Australia) of the dialysed graphite oxide for 2 to 3 h. Finally, centrifugation (3000 rpm for 30 min) was carried out to remove any unexfoliated graphite oxide.

2.3: Fabrication of LbL films of GO/PAH

First, the glass slides were cleaned by sonicating for 10 min in a solution containing 2:1(v/v) ratio of isopropanol and autoclaved water. GO (0.5 mg/mL) and PAH (1 mg/mL) solutions were prepared in autoclaved water and adjusted to pH 6. The pH of autoclaved water was also adjusted to that of the individual solutions for rinsing purpose in between each layer deposition. The multilayer films of GO/PAH were deposited according to the method described by Decher and co-workers.[42] The glass slides were dipped alternatively into PAH and GO solution for 30 min and rinsed three times with autoclaved water in between each layer deposition. The desired number of layers were coated by repeating each deposition cycle. All the solutions (PAH, GO and autoclaved water) were maintained at pH 6 throughout the experiment. The final layer was GO in all the cases.

2.4: Bacterial culture

A single isolated colony of *E. coli* K12 MG1655 was inoculated in 5 ml LB (Luria – Bertani) medium and grown at 37 ^{o}C and 250 rpm overnight. The bacterial culture was centrifuged at 6000 rpm for 10 minutes and the pellet was resuspended in PBS. The optical density was adjusted to 0.5 at 600 nm which corresponds to a concentration of 10^7 CFU/ml.

2.5: Antimicrobial activity of GO/PAH LbL films with *E. coli* culture

The thin film samples containing 20, 40 and 80 layers of GO/PAH were incubated in 15 mL of 0.5 OD bacterial suspension at 37 °C and 250 rpm and OD was measured after 4 and 16 h of incubation. A similar set of samples were exposed to laser and the growth was assessed by measuring OD after 4 and 16 h of incubation with conditions as above with appropriate control.

2.6: Photothermal therapy for killing the *E. coli* using GO/PAH films

For laser treatment of the cells along with GO/PAH films, a pulsed NIR-laser light at 1064 nm wavelength (Nd:YAG, with 10ns pulses, 10 Hz,) with fixed power (85 mW) was used. The laser illumination was performed by irradiating the laser source on the samples with and without GO/PAH films for 15 min. Samples were covered by thin coverslips in order to minimize the evaporation of the medium.

2.7: Live/Dead assay

A fluorescence-based cell viability assay was carried out to assess viable bacteria qualitatively based on previously reported studies.[28, 43] The cell suspensions treated with films for 4 h were exposed to propidium iodide (PI) (1 mg/mL) for 15 min to stain the dead cells with red fluorescence. The cells were then pelletized and washed with DI water. The live cells were then stained with DAPI for 5 min, which is a nucleic acid stain. The live and dead bacterial cells were visualized (under oil immersion 100X objective lens) with a confocal microscope (Olympus Fluorescence iX81).

3. Characterization Techniques

3.1: Scanning electron microscopy (SEM)

Both treated and untreated bacteria cell suspensions were dropped on silicon wafers and fixed with 2% glutaraldehyde. Then*, E. coli* was subjected to sequential treatment of 30, 50, 70, 80, 90 and 100% ethanol for dehydration. The dried samples were then sputter-coated with gold for imaging using scanning electron microscope equipped with field emission gun (FEI Sirion, Netherlands) at an operating voltage of 5 kV. The dried GO/PAH coated glass slide samples were coated with thin layer of gold before SEM analysis.

3.2: UV-Visible-NIR spectrophotometry

UV−visible-NIR absorption spectra of all the samples were measured on a Lambda 35 (Perkin-Elmer) spectrophotometer.

3.3: Confocal fluorescence microscope

The live/dead bacterial cells were visualized (under oil immersion 100× objective lens) with a confocal microscope (Olympus Fluorescence iX81).

3.4: Atomic Force Microscope

The atomic force microscopy (AFM) images of as exfoliated GO in the DI water suspension as well as prepared thin films of GO/PAH were taken with Nanosurf Easy Scan2 (Nanosurf AG, Switzerland) at room temperature.

4. Results and Discussion

4.1: Preparation of GO/PAH multilayer films

The fully exfoliated GO sheets were prepared using modified-Hummer's method and characterized similarly to our previous reports.[10, 11] Thickness measurement obtained from AFM (Figure S1, supplementary information) revealed that as prepared GO sheets contain one or two monolayers of GO in the aqueous suspension, since thickness of exfoliated sheets varied from ~1 to 2 nm.[40] The exfoliation of graphite oxide was also confirmed by TEM analysis as shown in Figure S2 (supplementary information). The excellent aqueous colloidal stability of GO aqueous suspension was supported by its high negative zeta potential (-34.0 mV). In the next step, LbL films were prepared by dipping the microscope glass slides alternatively into the suspensions of oppositely charged PAH and GO for fabricating thin films for depositing desired number of layers as demonstrated in the Figure 1. The coated films after each layer deposition were rinsed in autoclaved water to remove free or loosely adsorbed layer material. The driving force for the self-assembly of the GO/PAH layers onto negatively charged glass slide is the electrostatic attractive force exist between positively charged PAH and negatively charged GO at pH 6 as demonstrated in the GO/PAH hollow capsules synthesis.[10] To confirm, whether PAH and GO were being deposited under the experimental conditions, UV-visible-NIR absorbance spectra for each sample (20, 40 and 80 layers) was obtained from 300 and 1100 nm as shown in Figure 2A. The absorbance of the films did not increase linearly with increasing number of deposited GO/PAH layers (from 20 to 80). The irregular growth of the films could be attributed to the existence of gaps between the adjacently deposited GO sheets, or over-lapped patches and deposition of multiple GO sheets instead of monolayer GO as explained earlier in the case of LbL films of polyethylenimine(PEI)/TiO_2 nanosheets.[44] However, UV-vis-NIR results confirmed the regular stepwise growth of the films on the hydrophilic surface of the glass slides. The absorbance basically corresponds to GO, since PAH does not show any absorbance above 190

nm.[45] As shown in **Figure 2A**, there is a progressive increase in the absorbance band at 305 nm for GO/PAH films by increasing the number of layers from 20 to 80. The strong absorption band at 305 nm was attributed to n→π* transition of C=O bonds at the edges of GO as reported earlier in the case of GO/Poly(vinyl alcohol) LbL films.[46] Since glass absorbs light in the UV region and gives spurious peaks, the spectrum below 300 nm was not recorded.
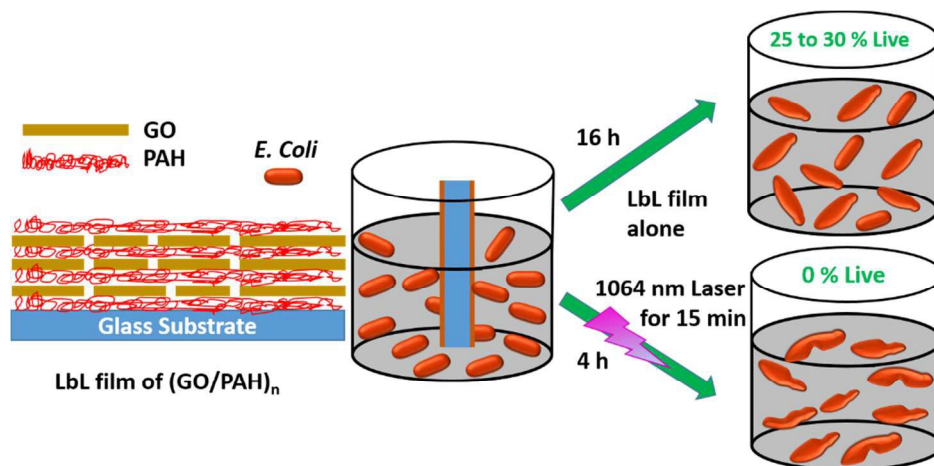

Figure 1: Schematic illustration of fabrication of LbL self-assembled films of (GO/PAH)$_n$ and study of their antimicrobial activity of those films with and without exposure of NIR-laser light in *E. coli* cells.

The optical photographs of prepared GO/PAH films deposited on clean glass substrates are shown in **Figure 2B.** The films appear flat and their transparency decreases (become more darker since GO is dark brown in colour) with increasing number of deposited layers from 20 to 80 indicating successful deposition of GO.[28] The SEM images (**Figure 3**) of GO/PAH film with 20 layers revealed its uniform and flat morphology, where GO sheets are visible on the surface as shown in high magnification images (**Figure 3B**). The morphology of the films and their thickness was characterized by AFM (**Figure 4)** which showed that the thickness of the films increased proportionally with increasing the number of layers from 20 to 80 layers.
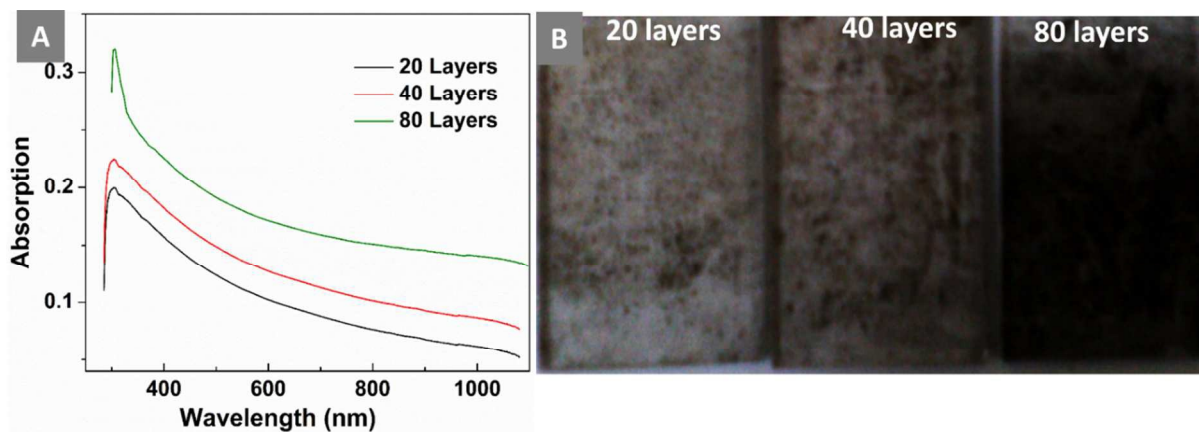
Figure 2: (A) UV-visible-NIR spectra of the GO/PAH films (20, 40 and 80 layers) and (B) The optical images of GO/PAH films of 20, 40 and 80 layers respectively.
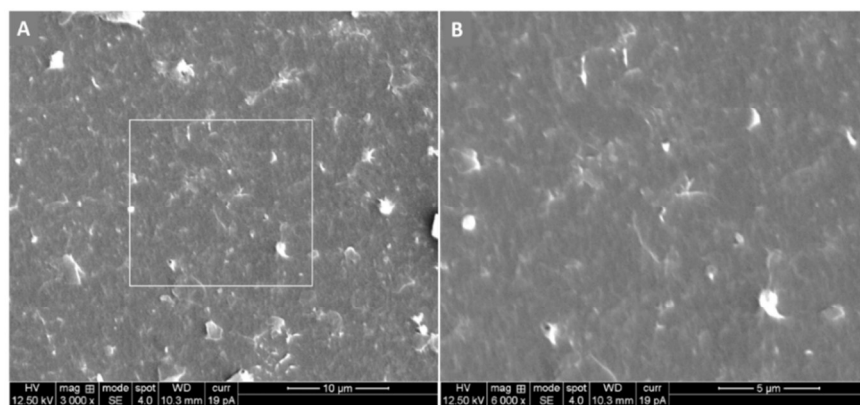

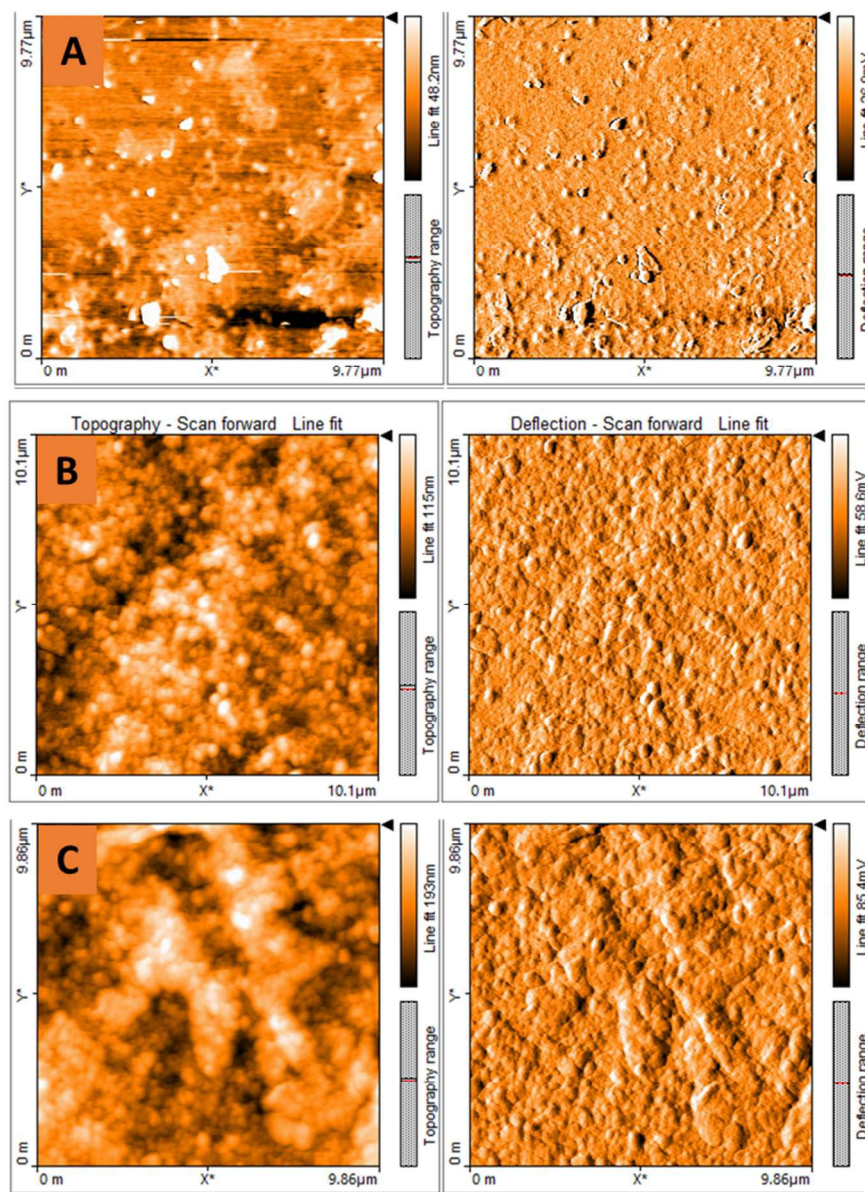**Figure 3:** Low and high magnification SEM images of GO/PAH films with 20 layers.

Figure 4: AFM images of the GO/PAH films (20, 40 and 80 layers) shown in A-C, respectively.

4.2: Antimicrobial activity of GO/PAH films with *E. coli*

We selected *E. coli K12* for antimicrobial studies, since it is known to be a multi-drug resistance bacterium.[47, 48] It has been reported that *E. coli K12* can grow in the presence of 1% sodium dodecyl sulfate as well as in several lipophilic antibiotics, such as penicillin G, erythromycin, fusidic acid, and rifamycin SV. In fact, a survey of recently reported antibiotics of natural origin showed that among those compounds which showed activity against gram-positive bacteria, more than 90% lacked activity at a useful level against *E. coli*.[48, 49] In addition, Akhavan et al. reported that the gram-negative *E. coli* bacteria with an outer membrane were

more resistant to the cell membrane damage caused by GO than other pathogens lacking the outer membrane.[50] They concluded that the more resistance of *E. coli* against the direct contact interaction with the nanowalls of GO as compared to gram-positive *S. aureus* could be assigned to the existence of an outer membrane in the structure of gram-negative *E. coli* and lack of such an outer membrane in the structure of gram-positive *S. aureus*.

The coated thin films with 20, 40 and 80 layers of GO/PAH were incubated in 15 ml of 0.5 OD *E. coli* culture (~ 10^7 CFU/mL) and absorbance was measured at 600 nm after 4 and 16 h incubation. From **Figure 5**, it can be seen that treating the bacterial culture with 20, 40 and 80 layers of GO/PAH films for 16 h decreased the viability of the culture to 74, 33 and 27% respectively in contrast to 80% in the control samples without films. Treating the bacterial culture with 20 layer films for 4 hours did not show significant decrease in viable cells. However, 40 and 80 layer films decreased the viability of the cells to ~ 40 and 36% respectively. This indicates that the GO/PAH films have antibacterial activity at higher concentrations of GO. The morphology of the 16 h treated cultures was studied using high resolution SEM as shown in **Figure 6A-6D**. It was observed that the control and 20-layer film treated cells were intact (**Figure 6A** and **6B**), whereas cells treated with 40 and 80 layer films showed a significant disrupted morphology as shown in **Figure 6C** and **6D** respectively. These results clearly support the antimicrobial activity of GO/PAH films and their activity is enhanced by increasing the number of layers. There are three kinds of mechanism for explaining the antimicrobial activity of carbon nanomaterials including GO. [33, 51, 52] First one is via membrane stress induced by direct physical contact between the sharp-edges (nanoknifes) of GO sheets and bacteria cell walls resulting in membrane perturbation and release of intracellular contents.[53, 54] Second one is by generating reactive-oxygen species (ROS) i.e. ROS-dependent oxidative stress[55] and third is ROS-independent oxidative stress, which results in disrupting a specific microbial process.[51] However, a recent study on LbL films of GO/titanate sheets revealed that antimicrobial activity of these hybrid GO films was mainly due to the membrane stress, where ROS-independent oxidative stress was minor and ROS-dependent oxidative stress was completely absent.[39, 54] In the case of GO/titanate sheets,[39] there was irreversible destruction of bacterial cell wall. A similar of kind cell wall damage was observed after treating *E. coli* with GO/PAH films containing 40 and 80 layers as shown in Figure 6C and 6D, respectively. Thus, the sanitization of *E.coli* by GO/PAH films could be mainly because of membrane stress caused on the cell walls

of bacteria, leading to damage of walls resulting in leakage of intracellular contents.[39, 53, 54] In addition, the gradual enhancement of antimicrobial activity of GO/PAH films with increasing number of layers could be due to the increase in the surface roughness of films as well as GO content. As obtained from AFM (Figure 4 and roughness values were shown in Figure S3-S5, ESI), the surface roughness (RMS) of 7.36, 18.45 and 39.24 nm was measured for 20, 40 and 80 layer films respectively. The increase in the roughness of films in turn offers facile adhesion of bacteria and enhances the antimicrobial activity of the films as explained previously for LbL films of GO/titanate nanosheets.[39, 54]
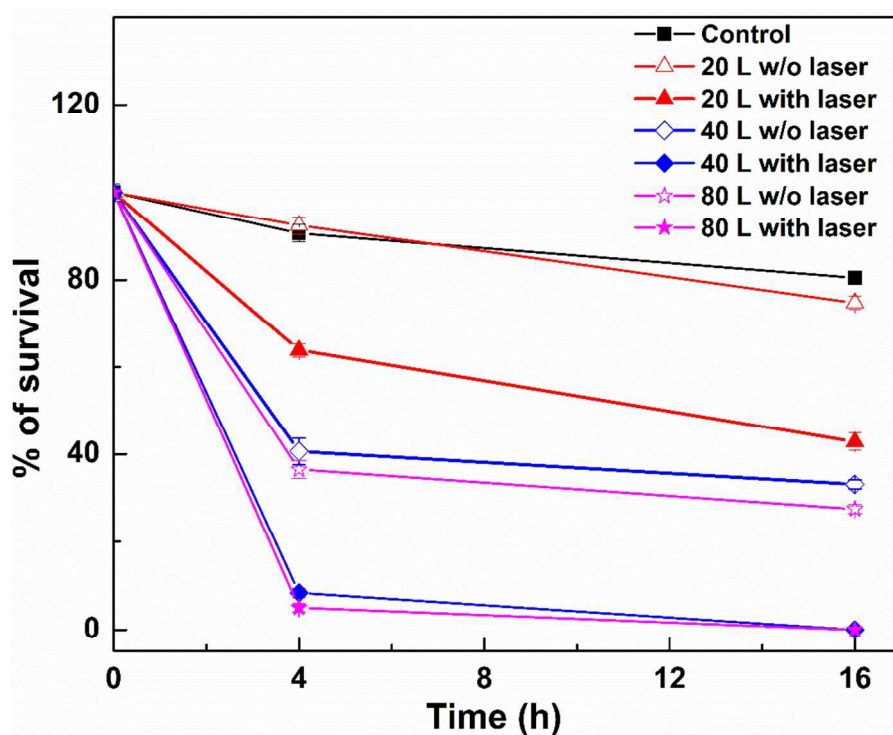

Figure 5: Shows the survivability of *E. coli* on treating LbL films of GO/PAH (20, 40 and 80 layers) with and without 1064 nm laser exposure, where control (black colour plot) represents only bacteria without any GO/PAH films with and without laser exposure.
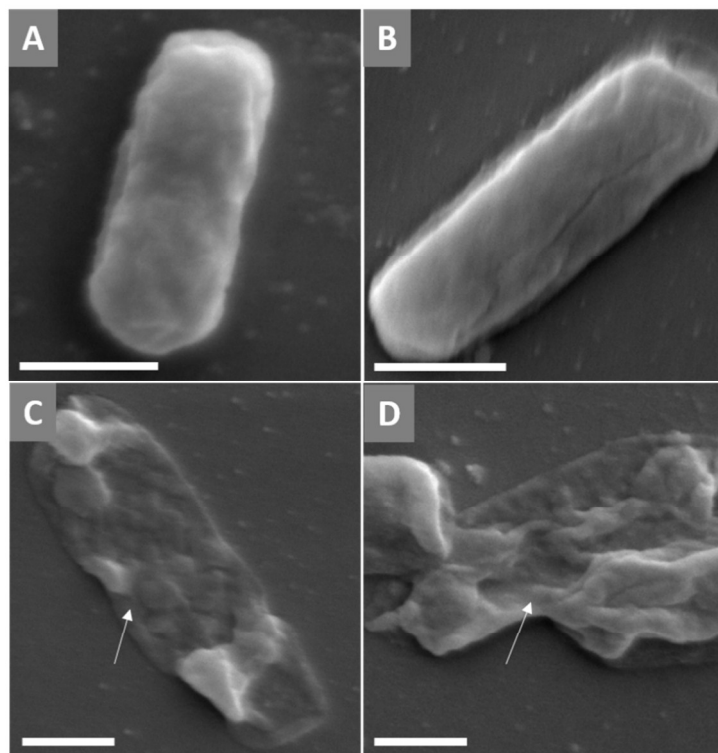
Figure 6: Shows SEM images of the control bacteria (A) and bacteria treated with GO/PAH films of 20, 40 and 80 layers respectively were shown in (B), (C) and (D) respectively. (Scale bars represents 500 nm in all the images)

In the next step, a similar set of 15 mL bacterial culture (0.5 OD) along with GO/PAH films (20, 40 and 80 layers) were exposed to pulse NIR-laser (Nd:YAG, 10 ns pulses with power of 85 mW) for 15 min and the absorbance was measured after 4 and 16 h incubation. As shown in **Figure 5**, after 16 h, 42% survivability was found in case of 20 layer films, while for 40 and 80 layer samples no bacteria survived. Increasing the number of deposited layers from 20 to 80 lead to an increase in NIR-light absorption as shown in UV-visible-NIR spectra **Figure 2**, which resulted in generation of higher local heating compared to the 20-layer film. Thus photothermal therapy (PTT) carried out with 40 and 80 layer films showed much higher antimicrobial activity compared to 20-layer film. Even for 4 h incubation, the cell viability was 63% for 20 layer, whereas 40 and 80 layered films showed less than 10% viability. Moreover, the control sample of bacterial culture without films after exposing to NIR-laser (85 mW) for 15 min, did not affect the viability of the bacteria (~ equal to control sample without any films). The applied power of NIR pulse laser (85 mW) is much lesser than the power required to kill *E. coli* using pulse

Nd:YAG laser (~100 W).[56] It clearly indicates that increased killing of bacteria by laser exposed film was because of photothermal effect of GO present in GO/PAH films.[25, 28]
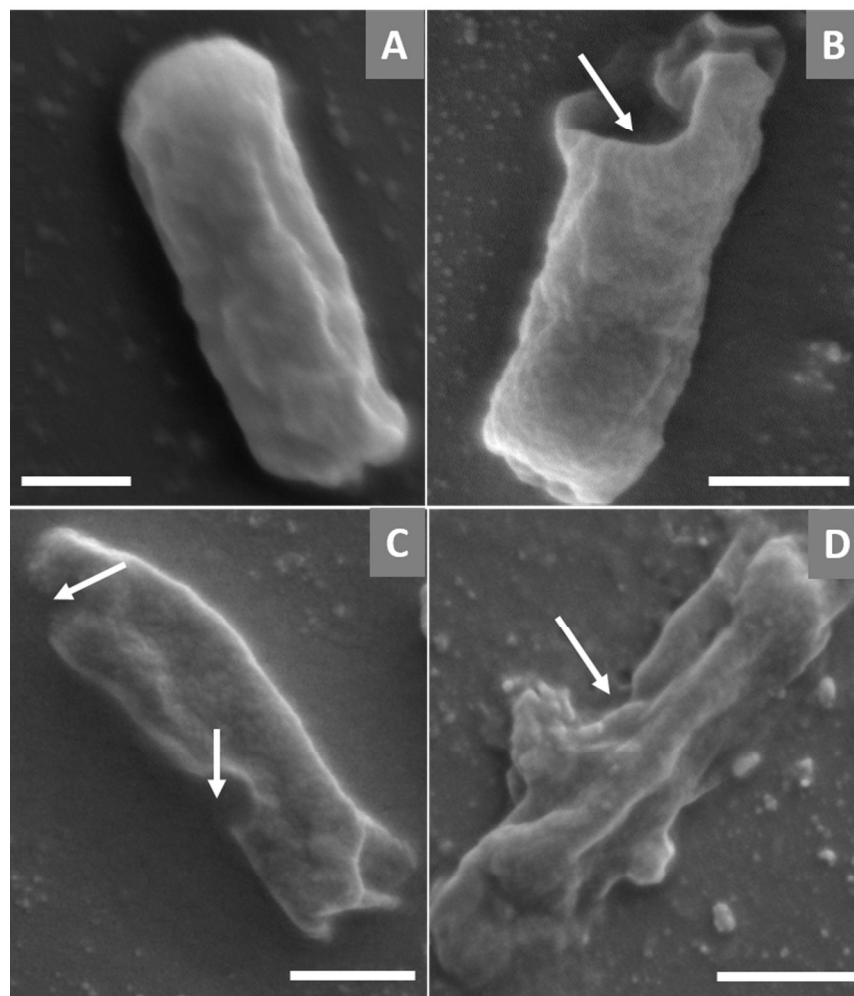

Figure 7: Shows SEM images (A) laser control bacteria and (B) to (D) show bacteria after NIR laser irradiation for 15 min using 20, 40 and 80 layer films respectively. (Scale bars represents 500 nm in all the images).

The incident laser light absorbed by GO/PAH films caused a local rise in temperature of more than ~ 100 °C within 15 min exposure, which was measured using a digital thermometer by immersing the thermometer into the falcon tube containing the GO/PAH films. For comparison, the temperature of ultrapure water treated with the same irradiation condition was also recorded and negligible heating of the solution without GO/PAH films was observed. The increase in the temperature could denature the enzyme and could inhibit necessary intracellular reactions, damage proteins and lipids on the cell membrane, and finally lead to bacterial death.[28] It is known that carbon allotropes such as graphene, GO and CNTs possess excellent photothermal

conversion ability under NIR-light exposure. GO has a higher photothermal conversion ability than CNTs.[28] The morphology and membrane integrity of *E .coli* cells with and without the NIR-laser exposure were examined by electron microscopy (**Figure 6-7 and Figure S6**). SEM images revealed that every bacterial cell membrane was disrupted indicated by the white arrows in both the Figures (6 and 7). When compared to the cells in the absence of NIR laser (**Figure 6**), the NIR-laser exposed cells clearly showed more damage to the cell-membrane as highlighted with white arrow marks (Figure 7). This cell-membrane damage could be due to bubble formation and photothermal disintegration.[28] In addition, there is a clear difference between the morphology of the cells treated with NIR-laser (Figure 7) and films alone as shown in **Figure 6**. Over all, the faster and better efficient killing of bacteria by GO/PAH films with help of NIR-laser treatment was attributed to the synergistic antimicrobial activity causing by the photothermal effect of GO sheets due to NIR laser irradiation and the mechanical stress induced by GO sheets. Since the bacteria was in physical contact with GO/PAH films for 4 or 16 h even after NIR-laser exposure for 15 min, there could be mechanical stresses induced onto bacteria in addition to photothermal heating by GO. Therefore, we believe that the efficient lysis of bacteria in the presence of NIR-laser could be the synergistic antimicrobial effect. On other hand, antimicrobial activity of PAH along could be negligible, since PAH can have antimicrobial activity against *E. coli* only at concentrations above 2.0 mg/mL in solution.[57] However, in the form of films with poly(acrylic acid), (PAH/PAA) showed negligible antimicrobial activity against *S. epidermidis.*[58] Thus, the antimicrobial activity of GO/PAH films is attributed primarily due to the presence of GO, which induces membrane stress or photothermal heating in the presence of NIR-laser. In addition, LbL films of GO can be fabricated with other cationic polymers like PEI. For instance, GO/PEI composite also showed good antimicrobial activity against *S. aureus* cells.[51]

4.3: Live/Dead assay

We further performed fluorescence-based live/dead assay to verify the viability of bacterial cells after incubation with GO/PAH films with and without pulse NIR-laser irradiation using confocal fluorescence microscope and results are shown in **Figure 8**. We carried out this fluorescence-based cell viability assay to verify the bacterial survivability based on the previously reported works. Elimelech and co-workers applied similar fluorescence dye methods to study the antimicrobial activity of SWCNTs and MWCTs,[43,59] and more recently Ling et al. also utilized the same method to check the antimicrobial activity of GO.[28] Membrane-

impermeant propidium iodide (PI) labels dead bacteria with red fluorescence, whereas membrane-permeant 4′-6-diamidino 2-phenylindole (DAPI) labels live bacteria with blue fluorescence.[28, 43] PI can only enter through damaged bacteria membranes and will be converted to a strongly red fluorescent dye through intercalating DNA.[4] On viewing through a fluorescence microscope, it was observed that most of the cells exposed to 40 and 80 layer films (**Figure 8C & 8D**) were stained red indicating that the PI dye penetrated inside the damaged cells while the 20 layer film (**Figure 8B**) treated samples had very few cells stained in red. The control sample (**Figure 8A**) however did not show any uptake of PI. It was also observed that the samples subjected to laser exposed films of 20, 40 and 80 layer (**Figure 8F-H**) showed an increased uptake of PI dye (red colour). These results are indicative of the physical disruption of the bacterial membrane by the GO/PAH films and consistent with that of the survival rates shown in **Figure 6** and **7**.
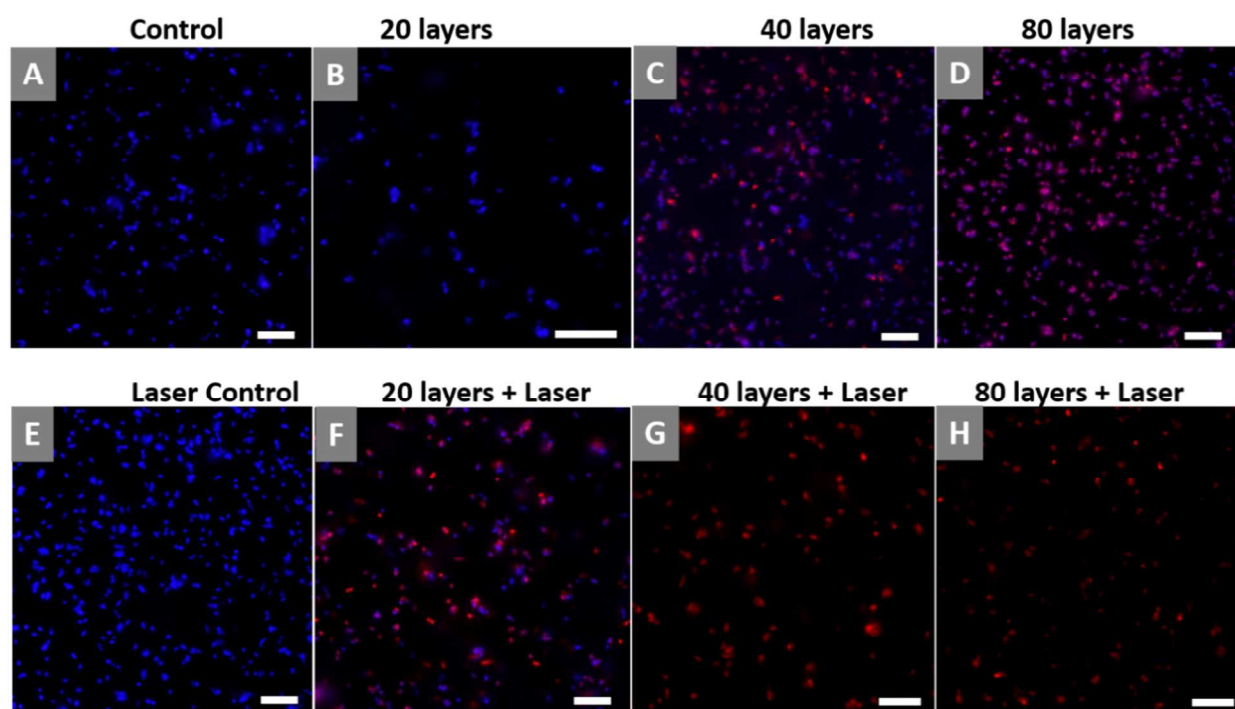

Figure 8: Confocal fluorescence microscope images of *E. coli* after treatment with (A) absence of GO/PAH films (B) to (D) shows the 20, 40, 80 layer films respectively and NIR-laser treated samples (E) laser light without films and (F)-(H) represents laser treated samples of 20, 40 and 80 layers respectively. (Scale bar in all the images represents 5 μm)

5: Conclusions

In summary, we have reported the first study on synergistic antimicrobial therapy for effective killing of *E. coli* by combining the intrinsic antimicrobial activity of GO sheets via induced membrane stress and the photothermal heating by GO due to NIR-laser exposure in the form of GO/PAH LbL multilayer films. GO/PAH composite films showed antimicrobial activity towards *E. coli* and their antimicrobial ability was enhanced by increasing the number of GO/PAH layers. The photothermal activity of these films showed an excellent sanitization efficiency with very low power NIR-pulse laser (Nd:YAG, 10 ns pulse, 85 mW) for 15 min. Finally, we have concluded that the synergistic antimicrobial effect (membrane stress + photothermal heating) caused more cell death as compared to only membrane stress inducing by incubation of GO/PAH films with bacteria. Thus, we strongly believe that these GO/PAH composite films system could be used for effective and efficient sanitization of other pathogenic bacteria. Further, these GO/PAH films can be coated as antimicrobial coatings over the any biomedical devices or implants or consumer products irrespective of their size and shape because of versatility of LbL films. In addition, the biocompatibility of graphene oxide/ PAH system makes it more beneficial for biomedical devices. In our future perspectives, we intend to test the sanitization of other bacteria and fungi with these GO/PAH films.

Acknowledgements

References

1. M. C. J. Bootsma, O. Diekmann and M. J. M. Bonten, *Proc. Natl. Acad. Sci. U.S.A.*, 2006, **103**, 5620-5625.
2. P. C. Ray, S. A. Khan, A. K. Singh, D. Senapati and Z. Fan, *Chem. Soc. Rev.*, 2012, **41**, 3193-3209.
3. P. Dallas, V. K. Sharma and R. Zboril, *Adv. Colloid Interface Sci.*, 2011, **166**, 119-135.
4. Y.-W. Wang, Y.-Y. Fu, L.-J. Wu, J. Li, H.-H. Yang and G.-N. Chen, *J. Mater. Chem. B*, 2013, **1**, 2496-2501.

RSC Advances Accepted Manuscript

5.   J. Borovička, W. J. Metheringham, L. A. Madden, C. D. Walton, S. D. Stoyanov and V. N. Paunov, *J. Am. Chem. Soc.*, 2013, **135**, 5282-5285.
6.   S. A. Khan, A. K. Singh, D. Senapati, Z. Fan and P. C. Ray, *Chem. Commun.*, 2011, **47**, 9444-9446.
7.   J.-W. Kim, E. V. Shashkov, E. I. Galanzha, N. Kotagiri and V. P. Zharov, *Lasers Surg. Med.*, 2007, **39**, 622-634.
8.   A. K. Geim, *Science*, 2009, **324**, 1530-1534.
9.   R. R. Nair, H. A. Wu, P. N. Jayaram, I. V. Grigorieva and A. K. Geim, *Science*, 2012, **335**, 442-444.
10.   R. Kurapati and A. M. Raichur, *Chem. Commun.*, 2012, **48**, 6013-6015.
11.   R. Kurapati and A. M. Raichur, *Chem. Commun.*, 2013, **49**, 734-736.
12.   X. Huang, X. Qi, F. Boey and H. Zhang, *Chem. Soc. Rev.*, 2012, **41**, 666-686.
13.   K. Yang, L. Feng, X. Shi and Z. Liu, *Chem. Soc. Rev.*, 2013, **42**, 530-547.
14.   N. Arya, A. Arora, K. S. Vasu, A. K. Sood and D. S. Katti, *Nanoscale*, 2013, **5**, 2818-2829.
15.   R. Kurapati, J. Russier, M. A. Squillaci, E. Treossi, C. Ménard-Moyon, A. E. Del Rio-Castillo, E. Vazquez, P. Samorì, V. Palermo and A. Bianco, *Small*, 2015, **11**, 3985-3994.
16.   A. Kundu, R. K. Layek and A. K. Nandi, *J. Mater. Chem.*, 2012, **22**, 8139-8144.
17.   W.-P. Xu, L.-C. Zhang, J.-P. Li, Y. Lu, H.-H. Li, Y.-N. Ma, W.-D. Wang and S.-H. Yu, *J. Mater. Chem.*, 2011, **21**, 4593-4597.
18.   D. Zhang, X. Liu and X. Wang, *J. Inorg. Biochem.*, 2011, **105**, 1181-1186.
19.   H. Unal and J. H. Niazi, *J. Mater. Chem. B*, 2013, **1**, 1894-1902.
20.   S. Park, N. Mohanty, J. W. Suk, A. Nagaraja, J. An, R. D. Piner, W. Cai, D. R. Dreyer, V. Berry and R. S. Ruoff, *Adv. Mater.*, 2010, **22**, 1736-1740.
21.   R. Chen, X. Zheng, H. Qian, X. Wang, J. Wang and X. Jiang, *Biomater. Sci.*, 2013, **1**, 285-293.
22.   T. S. Sreeprasad, M. S. Maliyekkal, K. Deepti, K. Chaudhari, P. L. Xavier and T. Pradeep, *ACS Appl. Mater. Interfaces*, 2011, **3**, 2643-2654.
23.   X.-N. Yang, D.-D. Xue, J.-Y. Li, M. Liu, S.-R. Jia, L.-Q. Chu, F. Wahid, Y.-M. Zhang and C. Zhong, *Carbohydr. Polym.*, 2016, **136**, 1152-1160.
24.   X. Cai, S. Tan, M. Lin, A. Xie, W. Mai, X. Zhang, Z. Lin, T. Wu and Y. Liu, *Langmuir*, 2011, **27**, 7828-7835.
25.   M. Acik, G. Lee, C. Mattevi, M. Chhowalla, K. Cho and Y. J. Chabal, *Nat. Mater.*, 2010, **9**, 840-845.
26.   B. Tian, C. Wang, S. Zhang, L. Feng and Z. Liu, *ACS Nano*, 2011, **5**, 7000-7009.
27.   S. P. Sherlock, S. M. Tabakman, L. Xie and H. Dai, *ACS Nano*, 2011, **5**, 1505-1512.
28.   M.-C. Wu, A. R. Deokar, J.-H. Liao, P.-Y. Shih and Y.-C. Ling, *ACS Nano*, 2013, **7**, 1281-1290.
29.   A. G. Skirtach, A. M. Yashchenok and H. Moehwald, *ChemInform*, 2012, **43**, DOI: 10.1002/chin.201211275.
30.   G. Cado, R. Aslam, L. Séon, T. Garnier, R. Fabre, A. Parat, A. Chassepot, J. C. Voegel, B. Senger, F. Schneider, Y. Frère, L. Jierry, P. Schaaf, H. Kerdjoudj, M. H. Metz-Boutigue and F. Boulmedais, *Adv. Funct. Mater.*, 2013, **23**, 4801-4809.
31.   J. Dai and M. L. Bruening, *Nano Lett.*, 2002, **2**, 497-501.
32.   T. Kruk, K. Szczepanowicz, D. Kręgiel, L. Szyk-Warszyńska and P. Warszyński, *Colloids Surf. B. Biointerfaces*, 2016, **137**, 158-166.
33.   S. Aslan, J. Maatta, B. Z. Haznedaroglu, J. P. M. Goodman, L. D. Pfefferle, M. Elimelech, E. Pauthe, M. Sammalkorpi and P. R. Van Tassel, *Soft Matter*, 2013, **9**, 2136-2144.
34.   C. Ye, Z. A. Combs, R. Calabrese, H. Dai, D. L. Kaplan and V. V. Tsukruk, *Small*, 2014, **10**, 5087-5097.
35.   J. Hong, K. Char and B.-S. Kim, *J. Phys. Chem. Lett.*, 2010, **1**, 3442-3445.
36.   T. Lee, S. H. Min, M. Gu, Y. K. Jung, W. Lee, J. U. Lee, D. G. Seong and B.-S. Kim, *Chem. Mater.*, 2015, **27**, 3785-3796.
37.   W. Qi, Z. Xue, W. Yuan and H. Wang, *J. Mater. Chem. B*, 2014, **2**, 325-331.

38.   J. D. Mangadlao, C. M. Santos, M. J. L. Felipe, A. C. C. de Leon, D. F. Rodrigues and R. C. Advincula, *Chem. Commun.*, 2015, **51**, 2886-2889.
39.   I. Y. Kim, S. Park, H. Kim, R. S. Ruoff and S. J. Hwang, *Adv. Funct. Mater.*, 2014, **24**, 2288-2294.
40.   N. I. Kovtyukhova, P. J. Ollivier, B. R. Martin, T. E. Mallouk, S. A. Chizhik, E. V. Buzaneva and A. D. Gorchinskiy, *Chem. Mater.*, 1999, **11**, 771-778.
41.   W. S. Hummers and R. E. Offeman, *J. Am. Chem. Soc.*, 1958, **80**, 1339-1339.
42.   G. Decher, *Science*, 1997, **277**, 1232-1237.
43.   S. Kang, M. Pinault, L. D. Pfefferle and M. Elimelech, *Langmuir*, 2007, **23**, 8670-8673.
44.   T. Sasaki, Y. Ebina, T. Tanaka, M. Harada, M. Watanabe and G. Decher, *Chem. Mater.*, 2001, **13**, 4661-4667.
45.   D. N. Priya, J. M. Modak and A. M. Raichur, *ACS Appl. Mater. Interfaces*, 2009, **1**, 2684-2693.
46.   X. Zhao, Q. Zhang, Y. Hao, Y. Li, Y. Fang and D. Chen, *Macromolecules*, 2010, **43**, 9411-9416.
47.   I. Ahmad and F. Aqil, *Microbiol. Res.*, 2007, **162**, 264-275.
48.   H. Nikaido, *J. Bacteriol.*, 1996, **178**, 5853-5859.
49.   H. G. Boman, K. Nordström and S. Normark, *Ann. N.Y. Acad. Sci.*, 1974, **235**, 569-586.
50.   O. Akhavan and E. Ghaderi, *ACS Nano*, 2010, **4**, 5731-5736.
51.   S. Liu, T. H. Zeng, M. Hofmann, E. Burcombe, J. Wei, R. Jiang, J. Kong and Y. Chen, *ACS Nano*, 2011, **5**, 6971-6980.
52.   Y. Zhang, S. F. Ali, E. Dervishi, Y. Xu, Z. Li, D. Casciano and A. S. Biris, *ACS Nano*, 2010, **4**, 3181-3186.
53.   W. Hu, C. Peng, W. Luo, M. Lv, X. Li, D. Li, Q. Huang and C. Fan, *ACS Nano*, 2010, **4**, 4317-4323.
54.   C. D. Vecitis, K. R. Zodrow, S. Kang and M. Elimelech, *ACS Nano*, 2010, **4**, 5471-5479.
55.   E. Cabiscol, J. Tamarit and J. Ros, *Int. Microbiol.*, 2000, **3**, 3-8.
56.   G. D. Ward, I. A. Watson, D. E. S. Stewart-Tull, A. C. Wardlaw, R. K. Wang, M. A. Nutley and A. Cooper, *J. Appl. Microbiol.*, 2000, **89**, 517-525.
57.   Y. Zhou, Y. Kong, S. Kundu, J. D. Cirillo and H. Liang, *J. Nanobiotechnology*, 2012, **10**, 19-28.
58.   A. Agarwal, T. L. Weis, M. J. Schurr, N. G. Faith, C. J. Czuprynski, J. F. McAnulty, C. J. Murphy and N. L. Abbott, *Biomaterials*, 2010, **31**, 680-690.
59.   S. Kang, M. S. Mauter and M. Elimelech, *Environ. Sci. Technol.*, 2008, **42**, 7528-7534.

Graphical Abstract
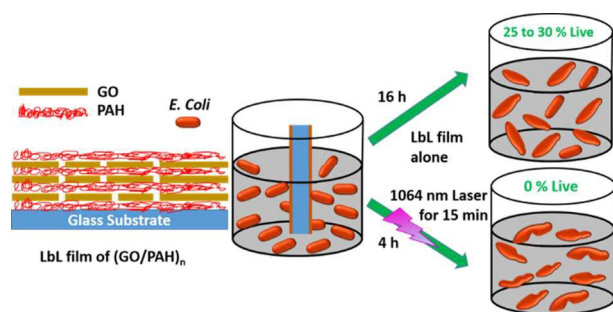
Simple and high-efficient synergistic antimicrobial coatings based on graphene oxide, which could be coated on any substrate irrespective of shape